Optimization-Based Remap

Denis Ridzal Pavel Bochev

Sandia National Laboratories

in collaboration with

Guglielmo Scovazzi (Sandia)

Mikhail Shashkov (LANL)

SIAM Conference on Computational Science and Engineering

February 28, 2011

Sandia National Laboratories is a multi-program laboratory managed and operated by Sandia Corporation, a wholly owned subsidiary of Lockheed Martin Corporation, for the U.S. Department of Energy's National Nuclear Security Administration under contract DE-AC04-94AL85000.

Outline

- Introduction to Remap
- Formulation of Optimization-Based Remap (OBR)
- Theoretical Properties of OBR
  - Mesh motion conditions for exact recovery of linear functions
  - Connection with Flux-Corrected Remap (FCR)
- Algorithms
- Three Instructive Examples
- Computational Studies

Introduction to Remap

Remap = Constrained Interpolation

Given: Discrete representation $\mathbf{f}_{\mathbf{A}}^{\mathbf{h}}$ of function $\mathbf{f}$ on mesh $\mathbf{A}$.

Find: *Accurate* discrete representation $\mathbf{f}_{\mathbf{B}}^{\mathbf{h}}$ of $\mathbf{f}$ on mesh $\mathbf{B}$, subject to physical constraints:

- conservation of mass, energy, etc.
- preservation of monotonicity
- physically meaningful ranges for variables: density ≥ 0, concentration $\in [0, 1]$

- Uses: transport algorithms, mesh rezone/repair, mesh tying.
- One flavor: Incremental remap $\rightarrow$ Mesh **A** is "close to" mesh **B**.
- Arbitrary Lagrangian-Eulerian (ALE) and Particle-In-Cell (PIC) methods depend on **robust remap algorithms**.

Challenge: Competing objectives and constraints!

Motivation for Optimization-Based Remap (OBR)

- balancing of desired mathematical features and physical constraints: accuracy vs. mass conservation, monotonicity, bounds on variables
- generality with respect to discretization: applicable to finite element, finite volume and finite difference schemes as well as particle methods; suitable for arbitrary polyhedral grids!

Liska, Shashkov, et al., in "Optimization-Based Synchronized Flux-Corrected Remap" (J. Comp. Phys. 2010) pursue a **local** optimization approach.

We have developed a new mathematical framework for the solution of incremental remap problems, based on a globally constrained optimization strategy.

Motivation for Optimization-Based Remap (OBR)

- balancing of desired mathematical features and physical constraints: accuracy vs. mass conservation, monotonicity, bounds on variables
- generality with respect to discretization: applicable to finite element, finite volume and finite difference schemes as well as particle methods; suitable for arbitrary polyhedral grids!

Liska, Shashkov, et al., in "Optimization-Based Synchronized Flux-Corrected Remap" (J. Comp. Phys. 2010) pursue a **local** optimization approach.

We have developed a new mathematical framework for the solution of incremental remap problems, based on a globally constrained optimization strategy.

We show that the global optimization formulation can have significant theoretical and practical advantages, at little or no added computational cost!

Problem Setup for Incremental Remap

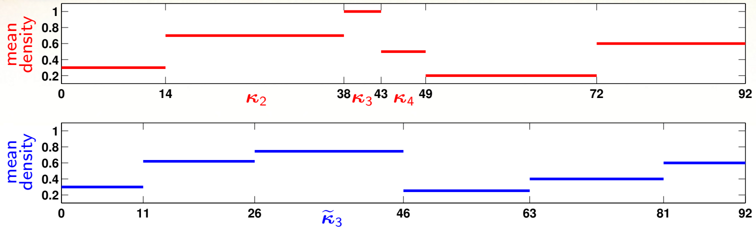

Notation:

- κ_i – cell in **old** grid, $\widetilde{\kappa}_i$ – cell in **new** grid; K is the number of cells
- $N(\kappa_i)$ – neighborhood of κ_i in old grid; $\mathcal{I}(N(\kappa_i))$ – neighbor indices
- **locality assumption**: $\widetilde{\kappa}_i \subset N(\kappa_i)$ for all $i = 1, \ldots, K$
- mean values of density on old mesh: $\rho_i = \int_{\kappa_i} \rho(\mathbf{x}) dV / V(\kappa_i)$
- masses: $m_i = \int_{\kappa_i} \rho(\mathbf{x}) dV$ or $m_i = \rho_i V(\kappa_i)$; total mass $M = \sum_{i=1}^{K} m_i$
- trivial observation: $\rho_i^{\min} \leq \rho_i \leq \rho_i^{\max} \quad \Leftrightarrow \quad \rho_i^{\min} V(\kappa_i) \leq m_i \leq \rho_i^{\max} V(\kappa_i)$, where $\rho_i^{\min}$ and $\rho_i^{\max}$ are the neighborhood minima and maxima

Problem Statement: Remap of Mass-Density

Given mean density values ρ_i on the old grid cells κ_i, find representations $\widetilde{m}_i$ for the masses on the new grid cells $\widetilde{\kappa}_i$,

$$\widetilde{m}_i \approx \widetilde{m}_i^{ex} = \int_{\widetilde{\kappa}_i} \rho(\mathbf{x}) dV \,; \quad i = 1, ..., K,$$

subject to the following requirements:

- **Mass conservation:** $\sum_{i=1}^{K} \widetilde{m}_i = \sum_{i=1}^{K} m_i = M\,.$
- **'Accuracy':** For a globally linear density $\rho(\mathbf{x})$, the remapped masses are exact in the following sense:

$$\widetilde{m}_i = \widetilde{m}_i^{ex} = \int_{\widetilde{\kappa}_i} \rho(\mathbf{x}) dV \,; \quad i = 1, \ldots, K\,.$$

- **Preservation of local bounds (implies monotonicity):**

$$\rho_i^{\min} \le \tilde{\rho}_i \le \rho_i^{\max} \;\text{ i.e. }\; \rho_i^{\min} V(\widetilde{\kappa}_i) = \widetilde{m}_i^{\min} \le \widetilde{m}_i \le \widetilde{m}_i^{\max} = \rho_i^{\max} V(\widetilde{\kappa}_i)\,.$$

Formulation of OBR

Optimization-Based Remap

- Express new masses via flux exchanges between old and new cells:

$$\widetilde{m}_i^{ex} = m_i + \sum_{j \in \mathcal{I}(N(\kappa_i))} F_{ij}^{ex} ,$$

$$\text{where } F_{ij}^{ex} = \int_{\widetilde{\kappa}_i \cap \kappa_j} \rho(\mathbf{x}) dV - \int_{\kappa_i \cap \widetilde{\kappa}_j} \rho(\mathbf{x}) dV .$$

- Exact mass fluxes are antisymmetric: $F_{ij}^{ex} = -F_{ji}^{ex} \rightarrow F_{ij} = -F_{ji}$
- Using these fluxes yields the approximation of the new cell masses

$$\widetilde{m}_i = m_i + \sum_{j \in \mathcal{I}(N(\kappa_i))} F_{ij} \quad \Rightarrow \quad \textbf{mass conservation}$$

- Assume that for every *old* cell κ_i there is a density reconstruction ρ_i^H that is exact for linear functions. Define **target fluxes** according to

$$F_{ij}^H = \int_{\widetilde{\kappa}_i \cap \kappa_j} \rho_i^H(\mathbf{x}) dV - \int_{\kappa_i \cap \widetilde{\kappa}_j} \rho_i^H(\mathbf{x}) dV .$$

Optimization-Based Remap

Reconcile preservation of linearity, mass and local bounds:

$$\min_{F_{ij}} \sum_{i=1}^{K} \sum_{j \in \mathcal{I}(N(\kappa_i))} (F_{ij} - F_{ij}^H)^2 \quad \text{subject to}$$

$$F_{ij} = -F_{ji} \qquad i = 1, \ldots, K, \;\; j \in \mathcal{I}(N(\kappa_i))$$

$$\widetilde{m}_i^{\min} \le m_i + \sum_{j \in \mathcal{I}(N(\kappa_i))} F_{ij} \le \widetilde{m}_i^{\max} \qquad i = 1, \ldots, K\,.$$

Enforce antisymmetry constraint by using only F_{pq} with $p < q$:

$$\min_{F_{ij}} \sum_{i=1}^{K} \sum_{\substack{j \in \mathcal{I}(N(\kappa_i)) \\ i<j}} (F_{ij} - F_{ij}^H)^2 \quad \text{subject to}$$

$$\widetilde{m}_i^{\min} \le m_i + \sum_{\substack{j \in \mathcal{I}(N(\kappa_i)) \\ i<j}} F_{ij} - \sum_{\substack{j \in \mathcal{I}(N(\kappa_i)) \\ i>j}} F_{ji} \le \widetilde{m}_i^{\max} \quad i = 1, \ldots, K.$$

Optimization-Based Remap

Reconcile preservation of linearity, mass and local bounds:

$$\min_{F_{ij}} \sum_{i=1}^{K} \sum_{j \in \mathcal{I}(N(\kappa_i))} (F_{ij} - F_{ij}^H)^2 \quad \text{subject to}$$

$$F_{ij} = -F_{ji} \qquad i = 1, \ldots, K, \;\; j \in \mathcal{I}(N(\kappa_i))$$

$$\widetilde{m}_i^{\min} \leq m_i + \sum_{j \in \mathcal{I}(N(\kappa_i))} F_{ij} \leq \widetilde{m}_i^{\max} \qquad i = 1, \ldots, K\,.$$

Enforce antisymmetry constraint by using only F_{pq} with $p < q$:

$$\min_{F_{ij}} \sum_{i=1}^{K} \sum_{\substack{j \in \mathcal{I}(N(\kappa_i)) \\ i<j}} (F_{ij} - F_{ij}^H)^2 \quad \text{subject to}$$

$$\widetilde{m}_i^{\min} \leq m_i + \sum_{\substack{j \in \mathcal{I}(N(\kappa_i)) \\ i<j}} F_{ij} - \sum_{\substack{j \in \mathcal{I}(N(\kappa_i)) \\ i>j}} F_{ji} \leq \widetilde{m}_i^{\max} \quad i = 1, \ldots, K.$$

A Taste of OBR

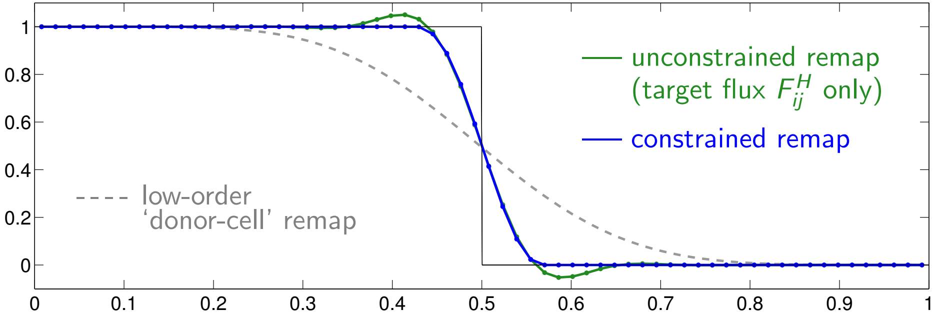

Theoretical Properties of OBR

Immediate Properties

$$\min_{F_{ij}} \sum_{i=1}^{K} \sum_{\substack{j \in \mathcal{I}(N(\kappa_i)) \\ i<j}} (F_{ij} - F_{ij}^H)^2 \quad \text{subject to}$$

$$\widetilde{m}_i^{\min} \leq m_i + \sum_{\substack{j \in \mathcal{I}(N(\kappa_i)) \\ i<j}} F_{ij} - \sum_{\substack{j \in \mathcal{I}(N(\kappa_i)) \\ i>j}} F_{ji} \leq \widetilde{m}_i^{\max} \quad i = 1, \ldots, K.$$

- Convex quadratic program.

- **Bound preservation (monotonicity)** is explicit as long as the feasible set defined by the inequalities is nonempty.
- **Theorem.** The feasible set of OBR is nonempty.

- **Optimally accurate** with respect to a set norm and a set target flux.
- Independent of dimension, cell topology and discretization.
- Separation of **accuracy** and **monotonicity**!
- Permits **additional physical bounds**.
- Extendible to **compatible remap of systems**.

- Mathematically "clean" formulation: **No flux limiting!**

Linearity Preservation

- **Theorem.** A **sufficient** condition for OBR to recover linear densities **exactly** is that the centroid of any new cell remain in the **convex hull** of the centroids of its old neighbors.

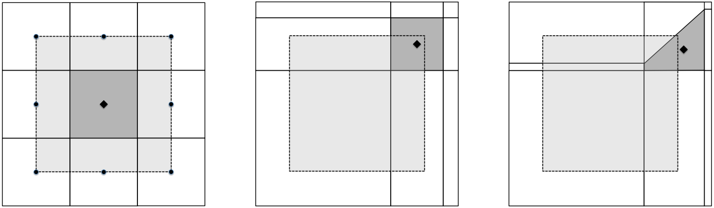

(a) original (b) admissible (c) inadmissible

- For example, less restrictive than Van Leer limiting (*B. Swartz*, "Good Neighborhoods for Multidimensional Van Leer Limiting", JCP, 1999, 154:237-241).

Connection with Flux-Corrected Remap (FCR)

Theorem. FCR can be formulated as a **global optimization problem**.

(1) The FCR cost function is equivalent to the OBR cost function.

(2) The FCR feasible set is **always a subset** of the OBR feasible set.

OBR

$$\min_{a_{ij}} \sum_{i=1}^{K} \sum_{\substack{j\in\mathcal{I}(N(\kappa_i))\\ i<j}} (1-a_{ij})^2 (dF_{ij})^2 \quad \text{subject to}$$

$$\widetilde{Q}_i^{\min} \leq \sum_{\substack{j\in\mathcal{I}(E(\widetilde{\kappa}_i))\\ i<j}} a_{ij}\, dF_{ij} - \sum_{\substack{j\in\mathcal{I}(E(\widetilde{\kappa}_i))\\ i>j}} a_{ji}\, dF_{ji} \leq \widetilde{Q}_i^{\max}$$

Admits a larger feasible set!

FCR

$$\min_{a_{ij}} \sum_{i=1}^{K} \sum_{\substack{j\in\mathcal{I}(N(\kappa_i))\\ i<j}} (1-a_{ij})^2 (dF_{ij})^2 \quad \text{subject to}$$

$$(a)\begin{cases} D_i^- \, dF_{ij} \leq a_{ij}\, dF_{ij} \leq 0 & \text{for } i<j,\ dF_{ij}\leq 0 \\ D_i^- \, dF_{ji} \geq a_{ji}\, dF_{ji} \geq 0 & \text{for } i>j,\ dF_{ji}\geq 0 \end{cases}$$

$$(b)\begin{cases} 0 \leq a_{ij}\, dF_{ij} \leq D_i^+ \, dF_{ij} & \text{for } i<j,\ dF_{ij}\geq 0 \\ 0 \geq a_{ji}\, dF_{ji} \geq D_i^+ \, dF_{ji} & \text{for } i>j,\ dF_{ji}\leq 0 \end{cases}$$

Algorithms

The Swept-Region Approximation

- OBR (and FCR) can be implemented using exact cell intersections.
- In 1D, we use exact cell intersections.
- In 2D, in order to avoid expensive geometric computations, we use the concept of swept regions (Margolin, Shashkov, JCP 2002).
- **OBR:** The swept-region flux approximation of F_{ij}^H is exact for linears.
- **FCR:** Blends F_{ij}^H and a monotone (provided exact cell intersections!) low-order reconstruction F_{ij}^L. Problem: The swept-region apprx. of F_{ij}^L is monotone *only under additional assumptions* on mesh motion.

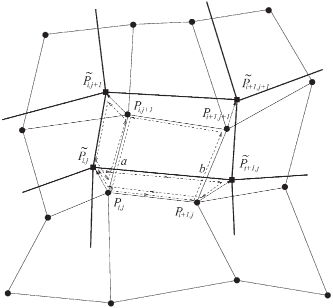

Margolin, Shashkov

Optimization Techniques

Primal OBR quadratic program:

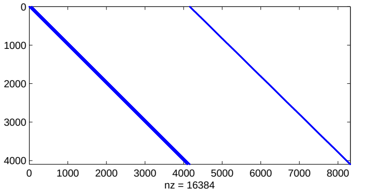

$$\begin{cases} \min\limits_{\vec{F}} \ \frac{1}{2}(\vec{F} - \vec{F}^H)^\mathsf{T}(\vec{F} - \vec{F}^H) \quad \text{subject to} \\ \vec{b}_{\min} \leq \mathbf{A}\vec{F} \leq \vec{b}_{\max} \end{cases}$$

Dual OBR quadratic program:

$$\begin{cases} \min\limits_{\vec{\lambda},\vec{\mu}} \ \frac{1}{2}\left(\mathbf{A}^\mathsf{T}\vec{\lambda} - \mathbf{A}^\mathsf{T}\vec{\mu}\right)^\mathsf{T}\left(\mathbf{A}^\mathsf{T}\vec{\lambda} - \mathbf{A}^\mathsf{T}\vec{\mu}\right) - \vec{\lambda}^\mathsf{T}\left(\vec{b}_{min} - \mathbf{A}\vec{F}^H\right) - \vec{\mu}^\mathsf{T}\left(-\vec{b}_{max} + \mathbf{A}\vec{F}^H\right) \\ \text{subject to} \quad \vec{\lambda} \geq 0, \ \ \vec{\mu} \geq 0 \end{cases}$$

- **Strong duality**, etc. imply $\vec{F}_* = \mathbf{A}^\mathsf{T}\vec{\lambda}_* - \mathbf{A}^\mathsf{T}\vec{\mu}_* + \vec{F}^H$.
- Use **reflective Newton method** by *Coleman and Li* (SIAM J. Opt. 1996): Newton iteration applied to a piecewise differentiable system that results from the first order optimality conditions for the dual problem.
- The quadratic term in the dual is governed by a symmetric positive semidefinite matrix; the computational cost of each Newton iteration is dominated by the solution of a well-structured sparse symmetric positive definite linear system (fast Cholesky factorizations) $\rightarrow \mathcal{O}(K)$ **algorithm**.

Three Instructive Examples

OBR preserves shape when FCR does not.

OBR preserves linear densities when FCR does not.

OBR preserves monotonicity when FCR does not.

OBR preserves shape when FCR does not.

Compressive Mesh Motion

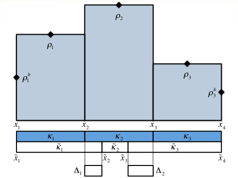

OBR Feasible Set (Cartoon)

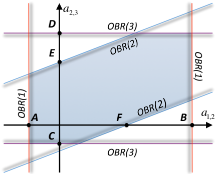

FCR Feasible Set (Cartoon)

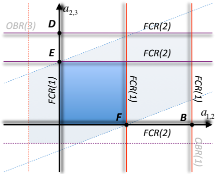

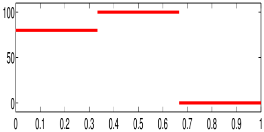

Original

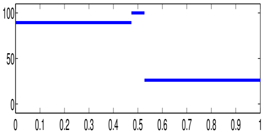

After a single OBR step

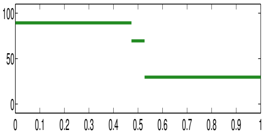

After a single FCR step

OBR preserves shape when FCR does not.

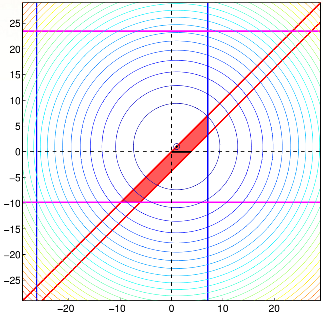

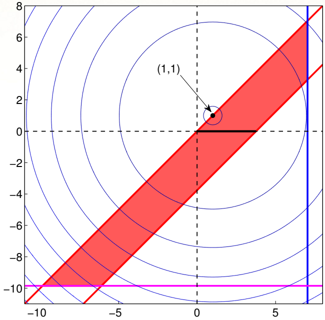

Figure: Level sets of the objective functional and the feasible sets for $\Delta_1 = \Delta_2 = 0.14$, $\rho_1 = 80$, $\rho_2 = 100$, $\rho_3 = 0$, and $\rho_1^b = \rho_3^b = 0$. The red region gives the OBR feasible set which contains the point $(1,1)$. The feasible set of FCR is given by the solid horizontal segment (black) and does not contain the point $(1,1)$. The right pane shows a zoom of the OBR and FCR feasible sets.

OBR preserves linear densities when FCR does not.

	$\ell = 7$	$\ell = 8$	$\ell = 9$	$\ell = 10$	$\ell = 100$	$\ell = 1000$
OBR (L_2 err)	**1.67e-16**	**0**	**3.20e-17**	**3.58e-17**	**1.63e-16**	**1.95e-14**
FCR (L_2 err)	**4.53e-17**	**3.58e-17**	2.32e-03	4.46e-03	2.09e-02	2.25e-02

Table: L_2 errors in the OBR and FCR remap of a linear density function in one dimension, for different compression ratios $\ell : 1$ of the middle cell.

OBR preserves monotonicity when FCR does not.

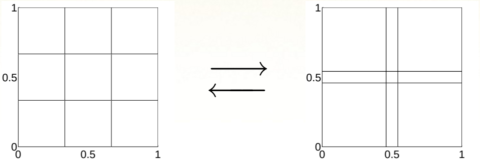

Figure: A 3×3 uniform initial grid (left pane) and the “compressed” grid (right pane) with a 4×4-fold compression of the middle cell.

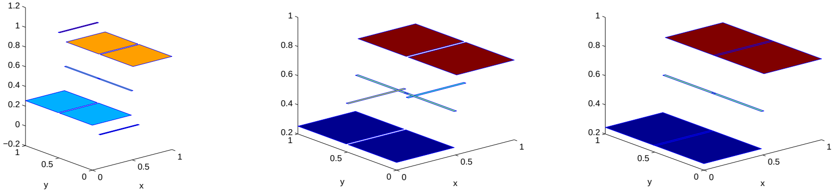

Figure: Linear density $\rho(x, y) = x$ remapped from the uniform 3×3 grid to the compressed “torture” grid with $\ell = 16$. Left to right: the donor-cell method, FCR, OBR. It is clear that OBR gives the best density approximation.

Computational Studies

Cyclic grids with small cell displacements.

Cyclic grids with large cell displacements.

Computational cost.

Small cell displacements

OBR							
#cells	#remaps	L_2 err	L_1 err	L_∞ err	L_2 rate	L_1 rate	L_∞ rate
64×64	320	6.58e-04	4.91e-04	5.78e-03	—	—	—
128×128	640	8.88e-05	6.16e-05	1.64e-03	2.89	3.00	1.82
256×256	1280	1.21e-05	7.82e-06	4.65e-04	2.88	2.99	1.82
512×512	2560	1.70e-06	9.89e-07	1.39e-04	2.87	2.98	1.80
FCR							
64×64	320	7.78e-04	4.95e-04	8.75e-03	—	—	—
128×128	640	1.22e-04	6.49e-05	2.81e-03	2.67	2.93	1.64
256×256	1280	2.00e-05	8.49e-06	8.89e-04	2.64	2.93	1.65
512×512	2560	3.43e-06	1.08e-06	2.84e-04	2.61	2.95	1.65

Table: OBR and FCR errors and convergence rate estimates for the **sine** density using 4 tensor-product cyclic grids. The L_2 and L_∞ rates for OBR are slightly better than those for FCR.

Small cell displacements

OBR							
#cells	#remaps	L_2 err	L_1 err	L_∞ err	L_2 rate	L_1 rate	L_∞ rate
64×64	320	9.12e-02	2.88e-02	4.72e-01	—	—	—
128×128	640	7.12e-02	1.75e-02	4.86e-01	0.36	0.72	-0.04
256×256	1280	5.57e-02	1.06e-02	4.87e-01	0.36	0.72	-0.02
512×512	2560	4.33e-02	6.35e-03	4.98e-01	0.36	0.73	-0.02
FCR							
64×64	320	8.43e-02	2.45e-02	4.67e-01	—	—	—
128×128	640	6.57e-02	1.47e-02	4.77e-01	0.36	0.73	-0.03
256×256	1280	5.12e-02	8.87e-03	4.77e-01	0.36	0.73	-0.02
512×512	2560	3.99e-02	5.34e-03	4.88e-01	0.36	0.73	-0.02

Table: OBR and FCR errors and convergence rate estimates for the **shock** density using 4 tensor-product cyclic grids. For this classical example, the convergence rates of OBR and M-OBR (FCR) are virtually identical.

Large cell displacements

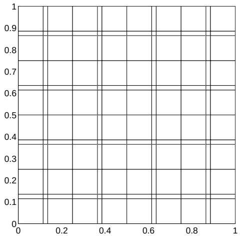

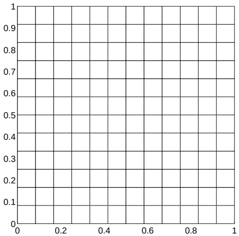

Figure: Grid deformation due to local compression (left pane) and the ‘repaired’ uniform grid (right pane).

Large cell displacements

OBR							
#cells	#remaps	L_1 err	L_2 err	L_∞ err	L_1 rate	L_2 rate	L_∞ rate
128×128	640	2.69e-04	3.65e-04	2.03e-03	—	—	—
256×256	1280	6.71e-05	9.08e-05	5.07e-04	**2.00**	**2.01**	**2.00**
512×512	2560	1.68e-05	2.27e-05	1.20e-04	**2.00**	**2.00**	**2.04**
1024×1024	5120	4.19e-06	5.66e-06	2.69e-05	**2.00**	**2.00**	**2.08**
FCR							
128×128	640	2.81e-04	3.47e-04	1.23e-03	—	—	—
256×256	1280	9.23e-05	1.19e-04	5.14e-04	1.61	1.54	1.26
512×512	2560	3.65e-05	5.05e-05	2.50e-04	1.47	1.39	1.15
1024×1024	5120	1.69e-05	2.39e-05	1.24e-04	1.35	1.28	1.10

Table: OBR and FCR errors and convergence rate estimates for the **sine** density using 4 cyclic repeated-repair grids. Rates expected of a second-order scheme are highlighted. It is evident that OBR delivers second-order accuracy, while FCR exhibits a trend toward a first-order scheme.

Large cell displacements

	$R = 213$	$R = 212$	$R = 211$	$R = 155$	$R = 154$	$R = 153$	$R = 100$	$R = 50$
OBR	**1.32e-13**	**1.42e-13**	**1.60e-13**	**4.60e-09**	4.06e-06	1.53e-05	1.97e-03	6.48e-03
FCR	**1.32e-13**	5.32e-08	1.10e-06	2.26e-03	2.35e-03	2.44e-03	5.73e+04	8.50e+11

Table: L_1 errors in the OBR and FCR remap of a linear density function on the 64×64 tensor-product grid, for different values of the pseudo-time step $1/R$. Errors smaller than 1e-8 are highlighted. OBR fails to preserve linear densities at $R = 154$, while FCR fails at $R = 212$, resulting in a pseudo-time step advantage for OBR of $212/154 \approx \mathbf{1.4}$. Beyond this point, OBR exhibits a graceful loss of accuracy; FCR becomes numerically unstable.

	$R = 25$	$R = 24$	$R = 23$	$R = 16$	$R = 15$	$R = 14$	$R = 10$	$R = 5$
OBR	**2.32e-14**	**4.49e-14**	**2.15e-13**	**4.52e-10**	4.14e-05	5.13e-04	1.16e-03	2.45e-03
FCR	**2.32e-14**	3.63e-07	1.67e-06	8.60e-04	1.16e-03	1.69e-03	5.74e-03	1.09e-02

Table: L_1 errors in the OBR and FCR remap of a linear density function on the 64×64 smooth nonorthogonal grid, for different values of the pseudo-time step $1/R$. Errors smaller than 1e-8 are highlighted. OBR fails to preserve linear densities at $R = 15$, while FCR fails at $R = 24$, resulting in a pseudo-time step advantage for OBR of $24/15 \approx \mathbf{1.6}$.

Computational Cost

# cells	# remaps	FCR(sec)	OBR(sec)	ratio
		Sine		
64×64	320	4.2	7.3	**1.7**
128×128	640	25.4	49.5	**1.9**
256×256	1280	176.5	390.6	**2.2**
512×512	2560	1812.5	3662.8	**2.0**
		Peak		
64×64	320	4.9	8.4	**1.7**
128×128	640	28.5	57.8	**2.0**
256×256	1280	183.8	418.6	**2.3**
512×512	2560	1832.9	4528.6	**2.5**
		Shock		
64×64	320	4.9	9.8	**2.0**
128×128	640	28.1	88.9	**3.2**
256×256	1280	184.7	438.6	**2.4**
512×512	2560	1794.1	3214.6	**1.8**

Table: Comparison of the computational costs of FCR and OBR, as measured by Matlab^{TM} wall-clock times on a single Intel Xeon X5680 3.33GHz processor, for density functions **sine**, **peak** and **shock** and the tensor-product cyclic grid. The cost of OBR is proportional, up to a modest constant, to the cost of FCR. The average cost ratio is only **2.1**.

Conclusions

- OBR is **monotone**, **conservative** and **linearity preserving** — and otherwise **optimally accurate** for a *fixed* norm and target flux.
- Independent of dimension, cell topology and discretization.
- OBR fully separates considerations of **accuracy** and **monotonicity**!
- Permits **additional physical bounds**.
- Extendible to **compatible remap of systems**.
- Mathematically "clean" formulation: **No flux limiting!**

Conclusions

- OBR is **monotone**, **conservative** and **linearity preserving** — and otherwise **optimally accurate** for a *fixed* norm and target flux.
- Independent of dimension, cell topology and discretization.
- OBR fully separates considerations of **accuracy** and **monotonicity**!
- Permits **additional physical bounds**.
- Extendible to **compatible remap of systems**.
- Mathematically "clean" formulation: **No flux limiting!**

- OBR is more robust and more accurate than local limiting (FCR).
- In the transport setting, OBR permits larger time steps.

Conclusions

- OBR is **monotone**, **conservative** and **linearity preserving** — and otherwise **optimally accurate** for a *fixed* norm and target flux.
- Independent of dimension, cell topology and discretization.
- OBR fully separates considerations of **accuracy** and **monotonicity**!
- Permits **additional physical bounds**.
- Extendible to **compatible remap of systems**.
- Mathematically "clean" formulation: **No flux limiting!**

- OBR is more robust and more accurate than local limiting (FCR).
- In the transport setting, OBR permits larger time steps.
- **Surprise:** Computational cost is comparable to local limiting (FCR).

Conclusions

- OBR is **monotone**, **conservative** and **linearity preserving** — and otherwise **optimally accurate** for a *fixed* norm and target flux.
- Independent of dimension, cell topology and discretization.
- OBR fully separates considerations of **accuracy** and **monotonicity**!
- Permits **additional physical bounds**.
- Extendible to **compatible remap of systems**.
- Mathematically "clean" formulation: **No flux limiting!**

- OBR is more robust and more accurate than local limiting (FCR).
- In the transport setting, OBR permits larger time steps.
- **Surprise:** Computational cost is comparable to local limiting (FCR).
- **However:** FCR performs well for small cell displacements and is ... a **local** (cell-wise) approximation of OBR → next talk!

Conclusions

- OBR is **monotone**, **conservative** and **linearity preserving** — and otherwise **optimally accurate** for a *fixed* norm and target flux.
- Independent of dimension, cell topology and discretization.
- OBR fully separates considerations of **accuracy** and **monotonicity**!
- Permits **additional physical bounds**.
- Extendible to **compatible remap of systems**.
- Mathematically "clean" formulation: **No flux limiting!**

- OBR is more robust and more accurate than local limiting (FCR).
- In the transport setting, OBR permits larger time steps.
- **Surprise:** Computational cost is comparable to local limiting (FCR).
- **However:** FCR performs well for small cell displacements and is ... a **local** (cell-wise) approximation of OBR → next talk!

- **Future:** remap of systems, various objective functions (norms and targets), remap of vector fields, use in ALE transport, use with nodal flux discretizations (Scovazzi), comparison with iterated FCR.